DOI: 10.1002/masy.200750832

Functional Opals from Reactive Polymers: Complex Structures, Sensors, and Modified Photoluminescence

Friederike Fleischhaker,[1,2] *Birger Lange,*[1] *Rudolf Zentel**[1]

Summary: This paper describes the synthesis and properties of functional opal structures, so-called colloidal photonic crystals (CPCs), from a variety of reactive polymers. Photoprocessable opals are presented as well as opals with incorporated "smart" defect layers that can be actively addressed by external stimuli. In addition, opals with functional bio-macromolecular defects have been developed. They present a new class of materials for optical biomonitoring through shifts of the induced photonic defect mode. Strong modification of photoluminescence according to the photonic bandstructure is observed from opals with embedded exclusively luminescent defect layer.

Keywords: colloids; luminescence; photonic crystal; sensors; stimuli-sensitive polymers

Introduction

Artificial opals represent a special sub-class of photonic crystals (PC), which are formed by self-assembly from inorganic or organic monodisperse colloids. Thus, they are also known as colloidal photonic crystals (CPC). Originally, opals were prepared from silica in analogy to their natural equivalents, but polymer-CPCs have received a lot of attention soon, due to their easy accessibility and the possibility for post-processing. For reviews see the following references.[1–3] This article focuses especially on functional opal-structures from reactive polymers and we present our latest research results regarding the aspects photo-patterning, controlled introduction of stimuli-responsive defects, biomonitoring, and modified photoluminescence.

The unique ability of PCs to manipulate the transmission of light may lead to potential applications ranging from simple optical switches to an optical computer. This requires the development of methods to incorporate designed defect structures into the crystal, though.

The flow of photons in PCs can be compared to the flow of electrons in semiconductors. Analogously to the local doping in semiconductors - the precondition for the creation of diodes, the controlled incorporation of defects in PCs is the precondition for the localization and guiding of photons.

Realizing defects in PCs, that are built in a top-down method fashion is rather straight forward and can be accomplished in one step during the fabrication of the matrix.[4–10] While these top-down methods are precise and allow design flexibility, they are often time-consuming and limited to small areas. Introduction of designed defect structures by low-cost and large-scale bottom-up self-assembly in 3D photonic crystals is only a recent development. The generation of advanced defects in CPCs is a complex matter, but great progress has been gained in the development of novel processes for the incorporation of point,[11,12] linear,[13–17] planar,[18–22] and 3D defects[23–28] during the last five years. Thus, large scale organization of monodisperse colloids can be combined

---

[1] Institute of Organic Chemistry, Department of Chemistry, Pharmacy and Earth Science, University of Mainz, Duesbergweg 10-14, 55128 Mainz, Germany
E-mail: zentel@uni-mainz.de
[2] Materials Chemistry Research Group, Chemistry Department, University of Toronto, 80 St. George Street, Toronto, Ontario, Canada, M5S 3H6

with controlled defect generation. The appearance of two recent review articles[29,30] details the efforts being taken in this direction.

Photo-Patterning

Colloidal crystals from inorganic materials such as silica or from polystyrene are limited in terms of chemical modifications, which can be used for patterning. Colloids based on various polymethacrylates possess the advantage that the corresponding CPCs can be structured by electron beam writing[11,14] or UV-lithography.[13,23] Such UV-processable monodisperse colloids have been synthesized from the acid labile polymer poly-*t*-butylmethacrylate (P*t*BMA). They can be loaded with photoacid generator and crystallized into polymer opal photonic crystals. Irradiation with UV-light followed by baking and development with aqueous base allows for subsequent patterning of the opaline films and the introduction of tailored defects.[13] Defect generation is thereby not limited to a planar opaline film. Defect structures can also be embedded into an opaline matrix, if a heterostructure of photosensitive and photostable spheres is used (see Figure 1).[23] To stabilize the system and to prevent the defects from collapsing, the photostable top-layer has to be mechanically stabilized. For this purpose core-shell colloids with a reactive outer shell containing epoxy-groups were developed that allow for temperature induced chemical crosslinking.[23]

It is possible to extend e-beam or nano-imprint techniques to define linear and other 2D defects in CPCs[11] by a multistep process. The direct (one step) incorporation of 3D defects into the interior of an artificial opal requires methods to initiate 3D resolved chemical reactions inside an opal like confocal microscopy[24,25] or more preferably two-photon lithography.[26,28]

By taking advantage of these techniques, defect structures can be fabricated directly inside the opal with control over all three dimensions using a two-photon sensitive photopolymerizable resin. As a host system both opals[24] and inverse opals[28] can be used. Inverted opals from the inorganic-organic hybrid polymer Ormocer® have the advantage of chemical and mechanical robustness and hence stay undamaged during the different processing steps (see Figure 2).[28]

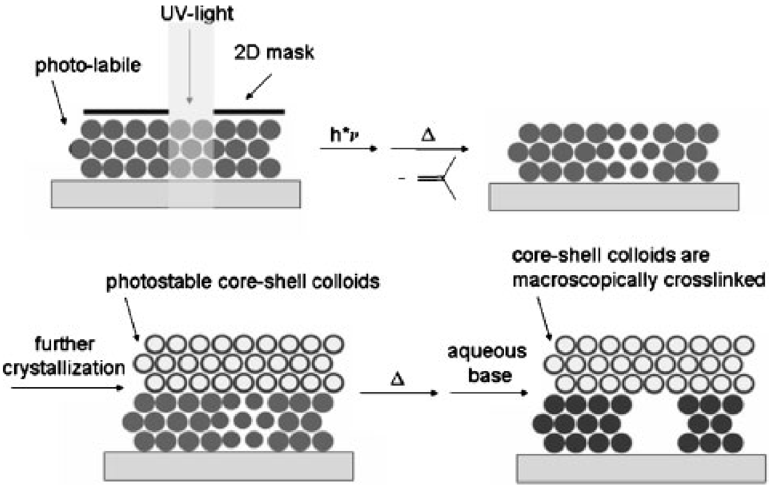

Figure 1.
Scheme for the construction of a 3D defect via multilayer build-up of photo-labile P*t*BMA colloids and core-shell-colloids, which can be thermally crosslinked.[23]

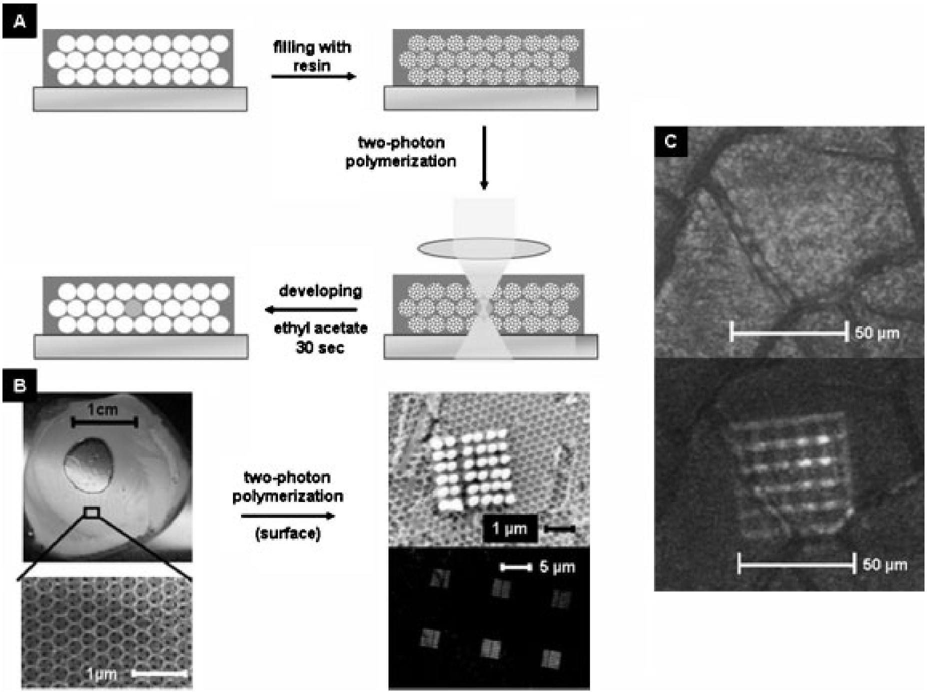

Figure 2.

A) Preparation of an inverse opal with 3D defects by two-photon lithography; B) Left: Digital photograph and electron microscopy image of an Ormocer® inverted opal; Right: electron microscopy and fluorescence microscopy image of luminescent defects introduced on the surface of the inverted opal using two photon lithography; C) Confocal microscope images of embedded luminescent defects in an Ormocer® inverted opal. Top: Surface of the inverted opal is focused. Bottom: Interior of the inverted opal is focused.[28]

Stimuli-Responsive Defects and Defects for Biomonitoring

Planar defect layers of different materials and with different chemical functionality have been embedded within CPCs by a number of bottom-up approaches. It has been shown that a monolayer of spheres sandwiched between two opal films made of spheres of different diameter can be prepared with the Langmuir-Blodgett technique and behaves as a two dimensional defect.[31–33] Spheres and various nanocrystalline aggregates that exceed the size of the CPC entrance windows have been incorporated as defect layers into CPCs by spin-coating.[34] Also, a synthesis method that enables the integration of dielectric planar defects in inverted CPCs using chemical vapour deposition (CVD) has been reported.[20,35]

Additionally, two bottom-up approaches have been developed that allow for the introduction of ''smart'' defect structures into CPC. In contrast to the previously described systems, these architectures can be actively addressed by various external stimuli. The defect is based on a functional thin film that is either prepared in a layer-by-layer (LbL) self-assembly fashion and microcontact transfer printing or by spin-coating and sacrificial CPC infiltration. Thus, it can consist of a wide range of charged or non-charged polymers, biopolymers, dyes, quantum dots, and other particles, to name a few.[21,22,36–38] This active element makes the materials interesting for applications as sensors, tunable filters, or tunable CPC-based laser sources.

In the first method (see Figure 3A), the functional thin film is LbL self-assembled onto a flat piece of polydimethylsiloxane

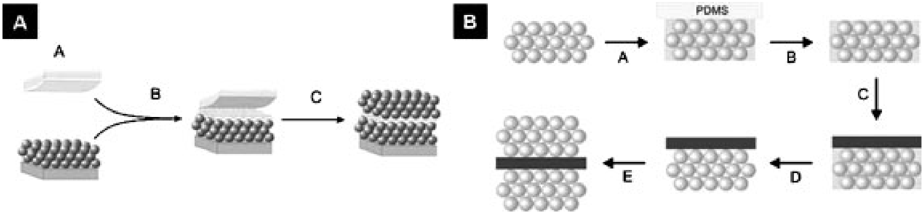

Figure 3.
Preparation techniques for embedding "smart" defect layers into CPCs (schematic illustration). A) Defect layer preparation based on LbL self-assembly and microcontact transfer printing.[36,37] B) Defect preparation by spin-coating and sacrificial sugar infiltration of the bottom-CPC.[38]

(PDMS), and the entire multilayer is microcontact transfer-printed onto the surface of a mechanically stabilized colloidal crystal. A second layer of CPC is then grown on top of this surface to form the embedded structural defect. In the second method (see Figure 3B), the defect layer is directly spin-coated on the surface of the bottom-CPC. To prevent penetration of the defect material into surrounding CPC voids during the spin-coating process, the bottom-CPC is melt-infiltrated with a sacrificial ribose filling. The sacrificial sugar filling is dissolved in water after spin-coating the defect film from all kind of hydrophobic solvents and the top-CPC is grown to complete the structure.

Optical spectra show a sharp transmission state within the photonic stopband induced by the defect (see Figure 4). The position of the defect state wavelength can be actively tuned by varying the thickness and/or refractive index of the defect layer using a photochemically active azobenzene based polymer,[21] a redox active polyferrocenylsilane (PFS) metallopolymer,[22] or a mechanically addressable thermoplastic elastomer.[38]

In addition, we developed CPCs with functional biomolecular planar defects. Bio-macromolecules such as proteins and DNA are embedded as nanometer thin sheets in a CPC, while maintaining both the bioactivity of these molecules and the optical properties of the CPC. It is shown that defect CPCs also present a new class of materials to optically monitor various aspects of chemistry or biochemistry taking place in the functional defect layer through precise shifts of the defect mode. DNA-

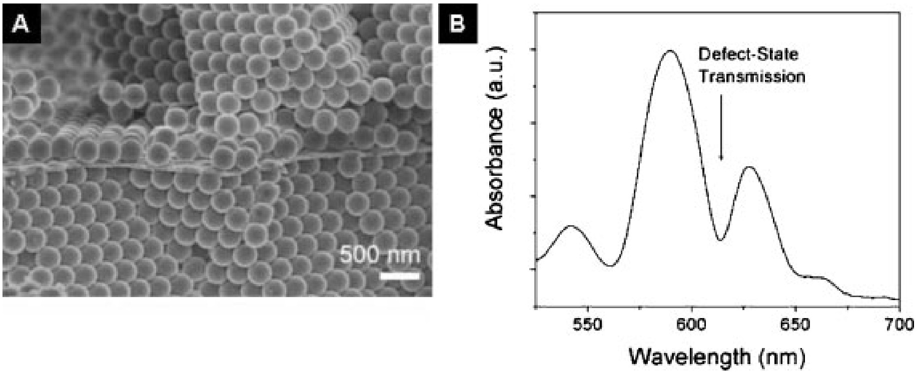

Figure 4.
A) Cross-sectional electron microscopy image of a CPC with embedded addressable azobenzene-based defect layer. Slight distortions in the structure result from the cleavage of the sample. B) Corresponding optical spectrum at normal incidence clearly showing photonic stopband and intragap defect transmission state.

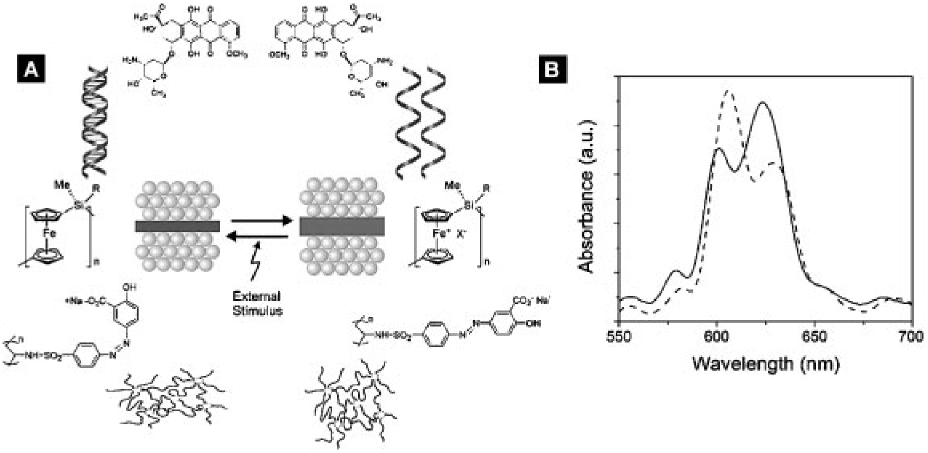

Figure 5.
A) Schematic illustration of various responsive defect materials inducing a change in the optical thickness of the defect layer when addressed by an external stimulus. B) Optical spectra exemplifying a shift of the intragap defect mode resulting from a change in thickness and/or refractive index of the defect layer.

based planar defect CPCs are used for example to demonstrate defect mode based optical monitoring of DNA conformational changes such as melting and annealing, as well as their enantioselective interaction with a chiral anti-cancer drug.[37] Optical characterization requires no sophisticated instrumentation and it is performed with a simple fiber optics spectrometer attached to an optical microscope. The setup allows for real time measurements and a spot size of less than 2 μm in diameter can be probed. The developed bio-defect CPCs are consequently highly suitable for array-based analysis and biochip applications. Since CPCs can be used for chromatography, the presented bio-defect CPCs are also potential candidates for combining separation and biomonitoring in a single microstructured sample.

Figure 5 graphically summarizes various responsive defect layer materials inducing optical shifts of the defect mode when addressed by an external stimulus.

Modified Photoluminescence

Using the spin-coating defect preparation method described in the previous section (Figure 3B), defect CPCs with a fluorescent dye located exclusively in the defect layer have been prepared and optically analyzed for the first time.[38]

Polymethylmethacrylate (PMMA) doped with the fluorescent dye 4-(dicyanomethylene)-2-methyl-6-(p-dimethyl-aminostyryl)-4H-pyran (DCM) is used as defect material.

The materials are chosen such that photoluminescence (PL) spectrum and photonic stopband including defect transmission state overlap. PL measurements show that the emission spectra of DCM incorporated in the defect layer of CPCs are strongly modified compared to the PL reference spectrum of DCM in a non-photonic organic polymer film. Strong suppression (~70–95%) of spontaneous emission at wavelengths of the photonic stopband is observed, and narrow luminescence peaks emerge at exactly the wavelengths of the defect transmission states (see Figure 6).

Comparisons to CPCs and defect CPCs infiltrated with light emitters demonstrate the modifying influence of the photonic bandstructure to be far more pronounced if the fluorophore is exclusively located within the defect layer and not distributed among the entire CPC structure. The most important reason for this observation is that light emitters located at or close to the

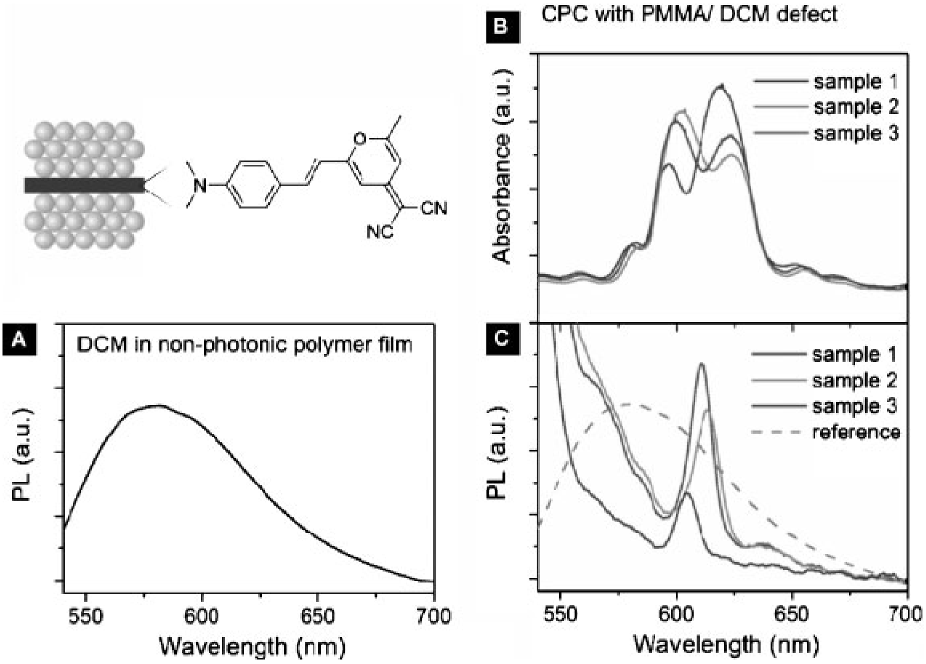

Figure 6.

CPC with DCM doped PMMA defect layer. A) Photoluminescence (PL) spectrum of DCM in a non-photonic organic polymer film (reference spectrum). Excitation wavelength: 532 nm. B) Transmission spectra of DCM doped PMMA defect layer CPCs with defect states at 604 nm, 615 nm and 611 nm, respectively (samples 1–3). C) PL spectra of DCM embedded in the defect layer of samples 1–3. Excitation wavelength: 532 nm.

detector-facing CPC surface of a defect CPC with random fluorophore distribution are not exposed to the photonic bandstructure in detection-direction. Hence, an average PL signal of modified and non-modified emission spectra is recorded.

Acknowledgements: The authors thank the DFG (Priority program: Photonic crystals) for financial support. Dr. F. Fleischhaker thanks the "Fonds der Chemischen Industrie" for a graduate scholarship, Prof. G. A. Ozin (University of Toronto) for the possibility to work in his lab and Dr. Jürgen Schmidtke (University of Freiburg) for support with photoluminescence measurements.

[1] Y. Xia, B. Gates, Y. Yin, Y. Lu, *Adv. Mater.* **2000**, *12*, 693; and special volume devoted to CPCs: *Adv. Mater.* **2001**, *13*, 369–534.

[2] C. Lopez, *Adv. Mater.* **2003**, *15*, 1679.

[3] M. Egen, R. Zentel, P. Ferrand, S. Eiden, G. Maret, F. Caruso, "Preparation of 3D photonic crystals from opals", in: *Photonic Crystals - Advances in Design, Fabrication and Characterization*, K. Busch, S. Lölkes, R. B. Wehrspon, H. Föll, Eds., Wiley-VCH, Weinheim **2004**, p. 109 ff.

[4] S. Noda, K. Tomoda, N. Yamamoto, A. Chutinan, *Science* **2000**, *289*, 604.

[5] A. Birner, R. B. Wehrspohn, U. M. Gosele, K. Busch, *Adv. Mater.* **2001**, *13*, 377.

[6] M. H. Qi, E. Lidorikis, P. T. Rakich, S. G. Johnson, J. D. Joannopoulos, E. P. Ippen, H. I. Smith, *Nature* **2004**, *429*, 538.

[7] G. Mertens, R. B. Wehrspohn, H. S. Kitzerow, S. Matthias, C. Jamois, U. Gösele, *Appl. Phys. Lett.* **2005**, *87*, 1108,

[8] K. K. Seet, V. Mizeikis, S. Matsuo, S. Juodkazis, H. Misawa, *Adv. Mater.* **2005**, *17*, 541.

[9] J. Scrimgeour, D. N. Sharp, C. F. Blanford, O. M. Roche, R. G. Denning, A. J. Turberfield, *Adv. Mater.* **2006**, *12*, 1557.

[10] S. Wong, M. Deubel, F. Perez-Willard, S. John, G. A. Ozin, M. Wegener, G. von Freymann, *Adv. Mater.* **2006**, *18*, 265.

[11] F. Jonsson, C. M. Sotomayor Torres, J. Seekamp, M. Schniedergers, A. Tiedemann, J. Ye, R. Zentel, *Microelectron. Eng.* **2005**, *78–79*, 429.

[12] Q. F. Yan, A. Chen, S. J. Chua, X. S. Zhao, *Adv. Mater.* **2005**, *17*, 2849.

[13] B. Lange, R. Zentel, C. K. Ober, S. Marder, *Chem. Mater.* **2004**, *16*, 5286.

[14] P. Ferrand, M. Egen, R. Zentel, J. Seekamp, S. G. Romanov, C. M. Sotomayor Torres, *Appl. Phys. Lett.* **2003**, *83*, 5289.

[15] B. H. Juarez, D. Golmayo, P. A. Postigo, C. López, *Adv. Mater.* **2004**, *16*, 1732.

[16] E. Vekris, V. Kitaev, G. von Freymann, D. D. Perovic, J. S. Aitchison, G. A. Ozin, *Adv. Mater.* **2005**, *17*, 1269.

[17] Q. F. Yan, Z. C. Zhou, X. S. Zhao, S. J. Chua, *Adv. Mater.* **2005**, *17*, 1917.

[18] P. Jiang, G. N. Ostojic, R. Narat, D. M. Mittleman, V. L. Colvin, *Adv. Mater.* **2001**, *13*, 389.

[19] K. Wostyn, Y. X. Zhao, G. de Schaetzen, L. Hellemans, N. Matsuda, K. Clays, A. Persoons, *Langmuir* **2003**, *19*, 4465.

[20] E. Palacios-Lidon, J. F. Galisteo-Lopez, B. H. Juarez, C. López, *Adv. Mater.* **2004**, *16*, 341.

[21] F. Fleischhaker, A. C. Arsenault, V. Kitaev, F. C. Peiris, G. von Freymann, I. Manners, R. Zentel, G. A. Ozin, *J. Am. Chem. Soc.* **2005**, *127*, 9318.

[22] F. Fleischhaker, A. C. Arsenault, Z. Wang, V. Kitaev, F. C. Peiris, G. von Freymann, I. Manners, R. Zentel, G. A. Ozin, *Adv. Mater.* **2005**, *17*, 2455.

[23] B. Lange, R. Zentel, C. K. Ober, *Poly. Prepr.* **2006**, *47*, 517.

[24] W. M. Lee, S. A. Pruzinsky, P. V. Braun, *Adv. Mater.* **2002**, *14*, 271.

[25] Y. H. Jun, C. A. Leatherdale, D. J. Norris, *Adv. Mater.* **2005**, *17*, 1908.

[26] S. A. Pruzinsky, P. V. Braun, *Adv. Funct. Mater.* **2005**, *15*, 1995.

[27] S. A. Pruzinsky, F. García-Santamaría, P. V. Braun, *PMSE Preprints.* **2006**, *94*, 99.

[28] B. Lange, R. Zentel, S. J. Jhaveri, C. K. Ober, Proceed. of SPIE, 61821W/1 **2006**.

[29] P. V. Braun, S. A. Rinne, F. García-Santamaría, *Adv. Mater.* **2006**, *18*, 2665.

[30] A. C. Arsenault, F. Fleischhaker, G. von Freymann, V. Kitaev, H. Migues, A. Mihi, N. Tetreault, E. Vekris, I. Manners, S. Aitchison, D. Perovic, G. A. Ozin, *Adv. Mater.* **2006**, *18*, 2779.

[31] M. Egen, R. Zentel, *Macromol. Chem. Phys.* **2004**, *205*, 1479.

[32] Y. Zhao, K. Wostyn, G. de Schaetzen, K. Clays, L. Hellemans, A. Persons, M. Szekeres, R. A. Schoonheydt, *Appl. Phys. Lett.* **2003**, *82*, 3764.

[33] P. Massé, S. Reculusa, K. Clays, S. Ravaine, *Chem. Phys. Lett.* **2006**, *422*, 251.

[34] R. Pozas, A. Mihi, M. Ocana, H. Miguez, *Adv. Mater.* **2006**, *18*, 1183.

[35] N. Tetreault, A. Mihi, H. Miguez, I. Rodriguez, G. A. Ozin, F. Meseguer, V. Kitaev, *Adv. Mater.* **2004**, *16*, 346.

[36] N. Tetreault, A. C. Arsenault, A. Mihi, S. Wong, V. Kitaev, H. Miguez, G. A. Ozin, *Adv. Mater.* **2005**, *17*, 1912.

[37] F. Fleischhaker, A. C. Arsenault, F. Peiris, V. Kitaev, I. Manners, R. Zentel, G. A. Ozin, *Adv. Mater.* **2006**, *18*, 2387.

[38] F. Fleischhaker, A. C. Arsenault, J. Schmidtke, R. Zentel, G. A. Ozin, *Chem. Mater.* **2006**, *18*, 5640.